

The Search for Neutrino Oscillations $\bar{\nu}_\mu \rightarrow \bar{\nu}_e$ with KARMEN

T.E. JANNAKOS

*Forschungszentrum Karlsruhe, Institut für Kernphysik,
D-76021 Karlsruhe, Postfach 3640, Germany
e-mail: thomas.jannakos@bk.fzk.de*

KARMEN, the **K**arlsruhe **R**utherford **M**edium **E**nergy **N**eutrino experiment, is located at the pulsed spallation neutron source ISIS of the Rutherford Appleton Laboratory. In the ISIS beam stop ν_μ , ν_e and $\bar{\nu}_\mu$ are produced from the $\pi^+-\mu^+$ decay chain at rest with energies up to 52.8 MeV. Besides a very low $\bar{\nu}_e$ contamination, ISIS stands out for its unique time structure. This allows for a highly sensitive search for $\bar{\nu}_\mu \rightarrow \bar{\nu}_e$ -oscillations with the KARMEN detector, a 56 t segmented liquid scintillation calorimeter with very good time, energy and position resolution. In 1996 an additional third veto counter was installed within the 7000 t steel blockhouse that shields the detector against cosmic induced background. Covering the detector from all sides it strongly reduces the background of cosmic induced high energy neutrons by a factor of 40. Here we present the data taken after this major upgrade from Feb. 1997 until Feb. 1999. Since there is no indication for any beam excess, an upper limit for the $\bar{\nu}_\mu \rightarrow \bar{\nu}_e$ oscillation is deduced using the Unified Approach based on a maximum likelihood analysis. The result, as all the data presented before, questions the interpretation of the LSND beam excess as an indication for $\bar{\nu}_\mu \rightarrow \bar{\nu}_e$ oscillation.

1 Introduction

The search for neutrino oscillations is one of the most fascinating topics of modern particle physics. The **K**Arlsruhe **R**utherford **M**edium **E**nergy **N**eutrino experiment KARMEN searches for neutrino oscillations in different appearance ($\nu_\mu \rightarrow \nu_e$ [2] and $\bar{\nu}_\mu \rightarrow \bar{\nu}_e$) and disappearance modes ($\nu_e \rightarrow \nu_x$ [3]). The physics program of KARMEN also includes the investigation of ν -nucleus interactions [4] as well as the search for lepton number violating decays of pions and muons and a test of the V-A structure of the μ^+ decay [5]. In the following we present the result of the search for $\bar{\nu}_\mu \rightarrow \bar{\nu}_e$ oscillation on the basis of the data taken from February 1997 until February 1999 (KARMEN 2 data) after the experiment upgrade in 1996. The data taken before the upgrade from 1990 - 1995 (KARMEN 1 data) is not included in the analysis. Such a combined analysis would yield a much lower sensitivity due to the relatively high cosmic induced neutron background of the KARMEN 1 data. In the data set presented here we measure the expected number of background events. Therefore we used the Unified Approach [6] based on a maximum likelihood analysis to derive a 90% confidence interval.

2 Neutrino Production and Detection

The KARMEN experiment utilizes the neutrinos produced by the neutron spallation source ISIS of the Rutherford Appleton Laboratory in Chilton, Oxon, UK. An intense beam (200 μ A) of protons is accelerated to an energy of 800 MeV by a rapid cycling synchrotron. The two parabolic proton pulses of 100 ns base width and a gap of 225 ns are produced with a repetition frequency of 50 Hz (duty cycle is 10^{-5}). The protons are stopped in the compact tantalum beam stop. Apart from spallation neutrons a large number of pions is produced and stopped immediately within the target. While almost all π^- undergo nuclear capture, the π^+ decay at rest (DAR) into μ^+ and ν_μ . The μ^+ are also stopped within the target and decay at rest via $\mu^+ \rightarrow e^+ + \nu_e + \bar{\nu}_\mu$. The minor fraction of π^- that decays in flight (0.65% relative to π^+ DAR) with an again suppressed subsequent μ^- decay leads to an extreme small $\bar{\nu}_e$ contamination of $\bar{\nu}_e/\nu_e \leq 6.2 \cdot 10^{-4}$ [7]. The energy spectra of the neutrinos are well defined due to the DAR of both the π^+ and μ^+ . The ν_μ from π^+ -decay is monoenergetic with $E(\nu_\mu)=29.8$ MeV; the continuous energy distributions up to 52.8 MeV of the ν_e and $\bar{\nu}_\mu$ can be calculated using the V-A theory and show the typical Michel shape. Therefore ISIS is a unique, isotropic source of ν_μ , ν_e and $\bar{\nu}_\mu$ from π^+ - μ^+ DAR that stands out for its time structure, the small $\bar{\nu}_e$ contamination and the well defined time and energy distribution of the produced neutrinos.

These neutrinos are detected with the KARMEN detector, a segmented calorimeter of 56 t of liquid scintillator. The matrix structure consists of 512 (32 rows \times 16 columns) optically independent modules with a cross section of 17.4×17.8 cm²

and a length of 353 cm. The segmentation is made of thin double acrylic walls separated by a small air gap. Every module is read out by two 3 inch photo tubes at each end. The position of an event within one module is given by the time difference between the photo tubes at both ends. The optimized optical properties of the organic liquid scintillator and an active volume of 96% result in an energy resolution of $\sigma_E = 11.5\%/\sqrt{E[MeV]}$. Gd_2O_3 coated paper within the module walls provides an efficient detection of thermal neutrons owing to the very high capture cross section of the $Gd(n, \gamma)$ reaction ($\sigma \approx 49000$ barn). The KARMEN electronics is synchronized to the ISIS proton pulses to an accuracy of 2 ns to fully exploit the time structure of the neutrinos. The detector is well protected against beam correlated background as well as the hadronic component of the cosmic radiation by a blockhouse made of 7000 t of steel. Cosmic muons entering or stopping close to the detector are identified by the two inner veto counters. The innermost veto covers the calorimeter from four sides and consists of modules identical to those of the calorimeter but half their width. The second veto counter is made of 136 plastic scintillator modules that shield the detector from five sides. With this configuration (KARMEN 1), the dominant background for the search for $\bar{\nu}_\mu \rightarrow \bar{\nu}_e$ oscillations were high energetic neutrons produced by cosmic muons within the steel blockhouse. To eliminate this background source an additional third veto counter made of 136 plastic scintillator modules with a total area of 300 m² was installed in 1996 [8]. It was placed right inside the steel blockhouse such that every muon is detected that could produce a neutron within the blockhouse at a distance of up to 1 m from the detector. With this configuration (KARMEN 2) cosmic induced background is considerably reduced by a factor of 40.

3 $\bar{\nu}_\mu \rightarrow \bar{\nu}_e$ oscillation signature

The probability for $\bar{\nu}_\mu \rightarrow \bar{\nu}_e$ oscillations can be written in a simplified 2 flavor description as

$$P(\bar{\nu}_\mu \rightarrow \bar{\nu}_e) = \sin^2(2\Theta) \cdot \sin^2\left(1.27 \frac{\Delta m^2 L}{E_\nu}\right) \quad (1)$$

where L is given in meters, E_ν is the neutrino energy in MeV, and Δm^2 denotes the difference of the squared mass eigenvalues $\Delta m^2 = |m_1^2 - m_2^2|$ in eV²/c⁴. The signature for the detection of a $\bar{\nu}_e$ is a spatially correlated, delayed coincidence of a positron from $p(\bar{\nu}_e, e^+)n$ with energies up to $E_{e^+} = E_{\bar{\nu}_e} - Q = (52.8 - 1.8) \text{ MeV} = 51.0 \text{ MeV}$ followed by the γ emission of either of the two neutron capture processes $p(n, \gamma)$ or $Gd(n, \gamma)$. The $p(n, \gamma)$ reaction leads to one γ with an energy of $E(\gamma) = 2.2 \text{ MeV}$ whereas the $Gd(n, \gamma)$ process leads to 3 γ in average with a sum energy of 8 MeV. The positrons are expected with a 2.2 μs exponential decrease of to the μ^+ decay after beam on target. The time difference between the positron and the capture γ is given by the thermalization and diffusion of the neutron.

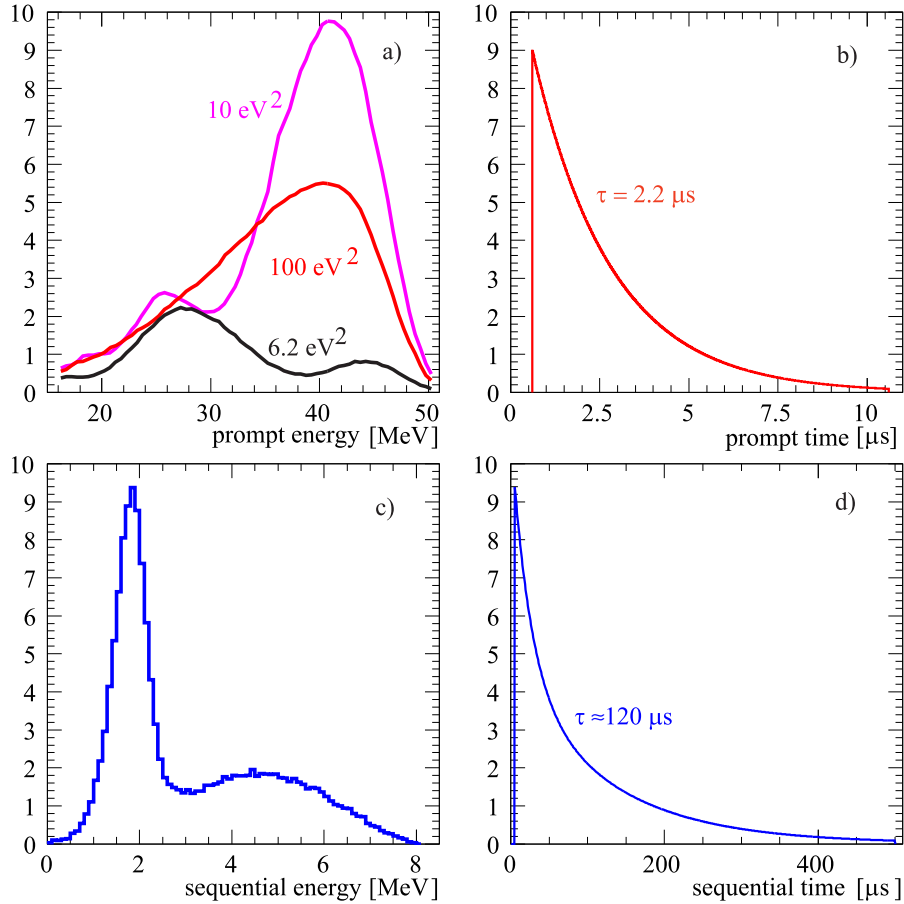


Figure 1: Signature of sequences of a positron (prompt event) and the correlated gammas from the neutron capture reaction (sequential event) that are expected for the $\bar{\nu}_\mu \rightarrow \bar{\nu}_e$ oscillation in the KARMEN detector: a) visible energy of the positron for three different values of Δm^2 as given by a Monte Carlo (MC) simulation; b) time of the positron relative to beam on target; c) visible energy of the delayed gammas from the nuclear neutron capture on either the free protons in the scintillator or the gadolinium in the segmentation; d) time difference of the neutron capture reaction relative to the positron.

To suppress cosmic induced background, a positron candidate is accepted only if there is no activity in the central detector and in both inner veto counters up to $24 \mu\text{s}$ before. When only the outermost third veto counter was hit, a dead time of $14 \mu\text{s}$ is applied.

The unique signature of the $p(\bar{\nu}_e, e^+)n$ reaction allows already for a strong discrimination of cosmic and neutrino induced background. The following cuts are introduced to maximize the sensitivity of the experiment: The positron has to be detected in a time window from $0.6 - 10.6 \mu\text{s}$ after beam on target with its energy in the range from $16 - 50 \text{ MeV}$. The sequential gamma must have an energy below 8 MeV and has to be correlated in space (within 1.2 m^3) and time ($5 - 300 \mu\text{s}$) to

the positron. For these cuts the total detection efficiency is – slightly depending on Δm^2 – approximately 20%. The expected signature for oscillation sequences in the KARMEN detector is shown in Fig. 1.

Table 1: Expected sequences from background reactions within the cuts specified above. Given are the mean values and their errors. Shown in the two last rows are the number of expected $p(\bar{\nu}_e, e^+)$ n reactions from the $\bar{\nu}_\mu \rightarrow \bar{\nu}_e$ oscillation for high Δm^2 ($= 100 eV^2$) assuming maximal mixing (i.e. $\sin^2(2\Theta) = 1$) and the number of actually measured sequences. All numbers are given for two different energy windows from 16 – 50 MeV and 36 – 50 MeV respectively.

Background reaction	events ($E \geq 16 \text{ MeV}$)	events ($E \geq 36 \text{ MeV}$)
$^{12}\text{C}(\nu_e, e^-)^{12}\text{N}_{\text{g.s.}}$ reaction	2.6 ± 0.3	0.00 ± 0.01
ν induced random coincidences	2.3 ± 0.3	0.09 ± 0.03
$\bar{\nu}_e$ contamination from ISIS	1.1 ± 0.1	0.31 ± 0.03
cosmic induced background	1.9 ± 0.1	0.56 ± 0.07
total expected background	7.8 ± 0.5	0.97 ± 0.08
measured sequences	8	0
$p(\bar{\nu}_e, e^+)$ n reactions for $\sin^2(2\Theta) = 1$	1605 ± 176	712 ± 78

4 Background Sources

One of the main advantages for the search of $\bar{\nu}_\mu \rightarrow \bar{\nu}_e$ oscillations with the KARMEN experiment is that the expected background is not only very small but also known with a high precision because most of it can be independently measured by applying different cuts. There are only four different sources of background:

- ν_e induced sequences caused by the charged current reaction $^{12}\text{C}(\nu_e, e^-)^{12}\text{N}_{\text{g.s.}}$ where the subsequent β decay of the $^{12}\text{N}_{\text{g.s.}}$ ($\tau = 15.9 \text{ ms}$) occurs within the first $300 \mu\text{s}$.
- Neutrino reactions that have a random coincidence with a low energy event from the natural radioactivity inside the detector.
- The small intrinsic $\bar{\nu}_e$ contamination from the $\pi^- - \mu^-$ decay chain in the ISIS target.
- Undetected cosmic muons which enter the detector or produce high energy neutrons via deep inelastic scattering in the inner part of the steel blockhouse.

The only background source not accessible to direct measurement is the $\bar{\nu}_e$ contamination. It is calculated using a detailed MC simulation of the ISIS target as well as all pion and muon production and decay or capture reactions [7]. Table 1 lists all background reactions and gives the number of expected events as well as their errors for the above defined cuts.

5 Maximum Likelihood Analysis

The maximum likelihood (ML) analysis is the most powerful method to infer the strength of a possible signal or to derive an upper limit if such a signal is not seen. Because of some advantages over other methods we use here the Unified Approach [6] recommended by the PDG [9] to derive a 90 % confidence interval from our ML analysis. For this ML analysis every background reaction and a possible oscillation signal are taken into account with their different probability density functions for the time and energy of the prompt event (the e^+) as well as the energy, and the time and position difference of the sequential event (the neutron capture) relative to the prompt event. The relative contributions of the individual background sources to the total number of background sequences is fixed whereas the number of oscillation sequences is allowed to vary freely. As an additional information, the likelihood function (LF) is weighted with a factor that is the conditional poisson probability of the number of inferred background sequences given the expectation value of the total background. The resulting LF depends on Δm^2 and $\sin^2(2\Theta)$ only, and thus for a given Δm^2 only on the number of oscillation sequences N_O inferred (or the number of background sequences N_B , for $N_B = N_{total} - N_O$).

For the Unified Approach we divided the relevant $[\Delta m^2; \sin^2(2\Theta)]$ parameter space in the interval $[(10^{-2}eV^2, 10^2eV^2); (10^{-4}, 1)]$ using a logarithmically equidistant grid of 90×72 points [10]. At every point on the grid we generate 8000 MC data samples according to the expected background and the given values of Δm^2 and $\sin^2(2\Theta)$ for this point. To these data samples the same ML analysis as to the experimental sample is applied. For every MC sample of this specific point on the grid one calculates the logarithm of the likelihoodratio $\Delta \log[L(\Delta m^2; \sin^2 2\Theta)]_{MC}$ of the value of the LF at its global maximum in the $[\Delta m^2; \sin^2(2\Theta)]$ parameter space to the value of the LF at the given point on the grid for which the sample was generated. This procedure gives a characteristic MC generated distribution of $\Delta \log[L(\Delta m^2; \sin^2 2\Theta)]_{MC}$ for every point on the grid which is then compared to the $\Delta \log[L(\Delta m^2; \sin^2 2\Theta)]_{EXP}$ value of the experimental data set (i.e. the logarithm of the ratio of the experimental LF at its global maximum to its value at a given point on the grid). The 90 % confidence interval (C.I.) is the set of points on the grid for which the experimental value $\Delta \log[L(\Delta m^2; \sin^2 2\Theta)]_{EXP}$ is smaller than at least 10 % of all MC generated $\Delta \log[L(\Delta m^2; \sin^2 2\Theta)]_{MC}$ (see Fig. 2). If, on the other hand, for given parameters $[\Delta m^2; \sin^2(2\Theta)]$ $\Delta \log[L(\Delta m^2; \sin^2 2\Theta)]_{EXP}$ lies in the upper 10 % tail of the MC distribution this point on the grid does not belong to the 90 % confidence interval. The upper 90 % confidence limit (C.L.) as shown in Fig. 4 is the upper limit of the 90 % C.I.. The interpretation of this C.L. is that for all parameter combinations Δm^2 and $\sin^2(2\Theta)$ on this curve 90 % of a large number of hypothetical KARMEN experiments would have seen a larger “signal” (i.e. *smaller* $\Delta \log[L(\Delta m^2; \sin^2 2\Theta)]_{EXP}$) than the one actually observed if – and this is important

– the true parameters of the $\bar{\nu}_\mu \rightarrow \bar{\nu}_e$ oscillation were in this region of the parameter space.

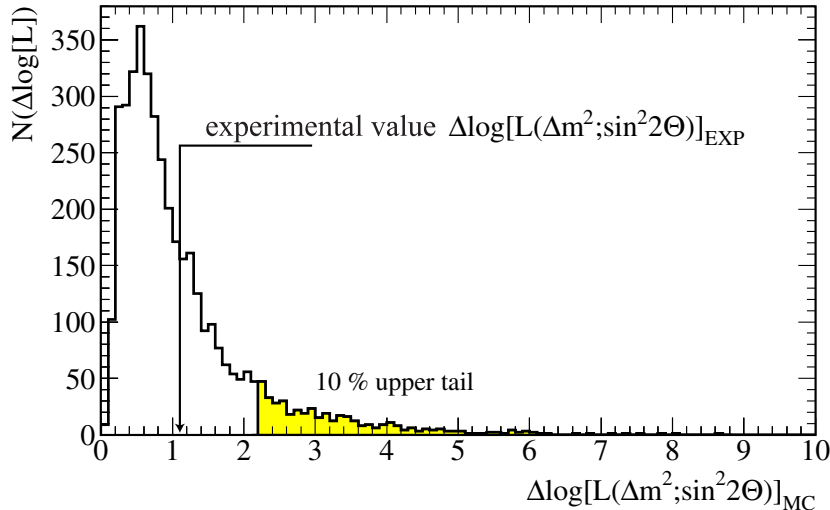


Figure 2: Monte Carlo generated distribution of the logarithm of the likelihoodratios $\Delta\log[L(\Delta m^2; \sin^2 2\Theta)]_{MC}$ for $\Delta m^2 = 100 \text{ eV}^2$ and $\sin^2(2\Theta) = 0.001$. The experimental value $\Delta\log[L(\Delta m^2; \sin^2 2\Theta)]_{EXP}$ for this point in the parameter space is to the left of the upper 10 % tail of the MC distribution. Therefore this parameter combination belongs to the 90 % C.I..

6 Results and Conclusion

The results presented here are based on the data recorded in the measuring period from February 1997 to February 1999 which corresponds to 4670 C protons on target. Within the cuts defined in Sect. 3 we find 8 sequences as shown in Fig. 3. Since we expect a total background of 7.8 ± 0.5 sequences there is absolutely no indication for a beam excess. For this data set the above described analysis leads to a 90 % C.L. of $\sin^2(2\Theta) = 2.1 \cdot 10^{-3}$ for large Δm^2 (i.e. 100 eV^2). The 90 % C.L. as a function of Δm^2 can be seen in Fig. 4. Also shown is the sensitivity of the KARMEN experiment. The sensitivity of an experiment is defined as the mean confidence limit a large number of identical experiments would yield if there was no oscillation. The actual limit is slightly “better” than the sensitivity with $\sin^2(2\Theta) = 2.3 \cdot 10^{-3}$ for large Δm^2 . Naively one would expect that the sensitivity is at slightly lower $\sin^2(2\Theta)$ than the exclusion curve and not vice versa because we measure more events (0.2) than the expected background. This apparent contradiction is explained by the fact that there are no events above 36 MeV where – depending on Δm^2 – roughly half of all oscillation sequences should be and only 0.97 ± 0.08 background events are expected (see Tab. 1). This leads also to an LF that has its global maximum in the region of small negative $\sin^2(2\Theta)$ which - for a null result - is as possible as a global

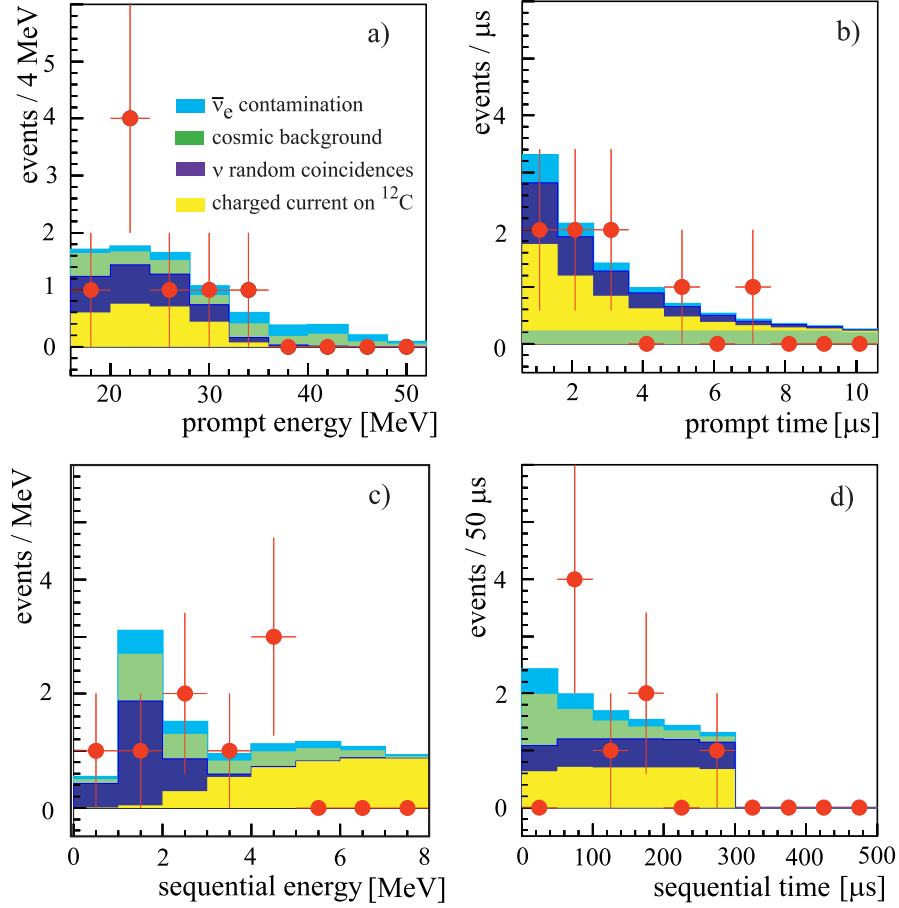


Figure 3: Distribution of the expected background sequences for the prompt energy (a) and time (b) distribution as well as the sequential energy (c) and time (d) distribution. Also shown are the 8 measured sequences which agree nicely in their shape with the expected background.

maximum in the region of positive $\sin^2(2\Theta)$. The 90% C.L. from our ML analysis is compared in Fig. 4 to the LSND result [11]. It excludes most of the LSND favoured region and is thus – as is the fact that there is no event above 36 MeV – strongly questioning the interpretation that the LSND beam excess is an indication for $\bar{\nu}_\mu \rightarrow \bar{\nu}_e$ oscillations. Furthermore one has to keep in mind that the KARMEN limit that was derived from the Feb.97 - Apr.98 data set and that is also shown in Fig. 4 puts an even stronger constraint on the LSND favoured region. In this data set (which had slightly different cuts) we expected 2.9 ± 0.1 background sequences and measured no event at all. This yields, using again the unified approach, a 90% C.L. of $1.3 \cdot 10^{-3}$ for large Δm^2 and a sensitivity of $5.4 \cdot 10^{-3}$, respectively [12], [13]. Although this limit was criticized by some people, it is of course valid and correct: If one accepts the ansatz of the Unified Approach one must NOT argue that this (“lucky”) limit is not trustworthy for this would mean to reduce the Unified Approach to absurdity.

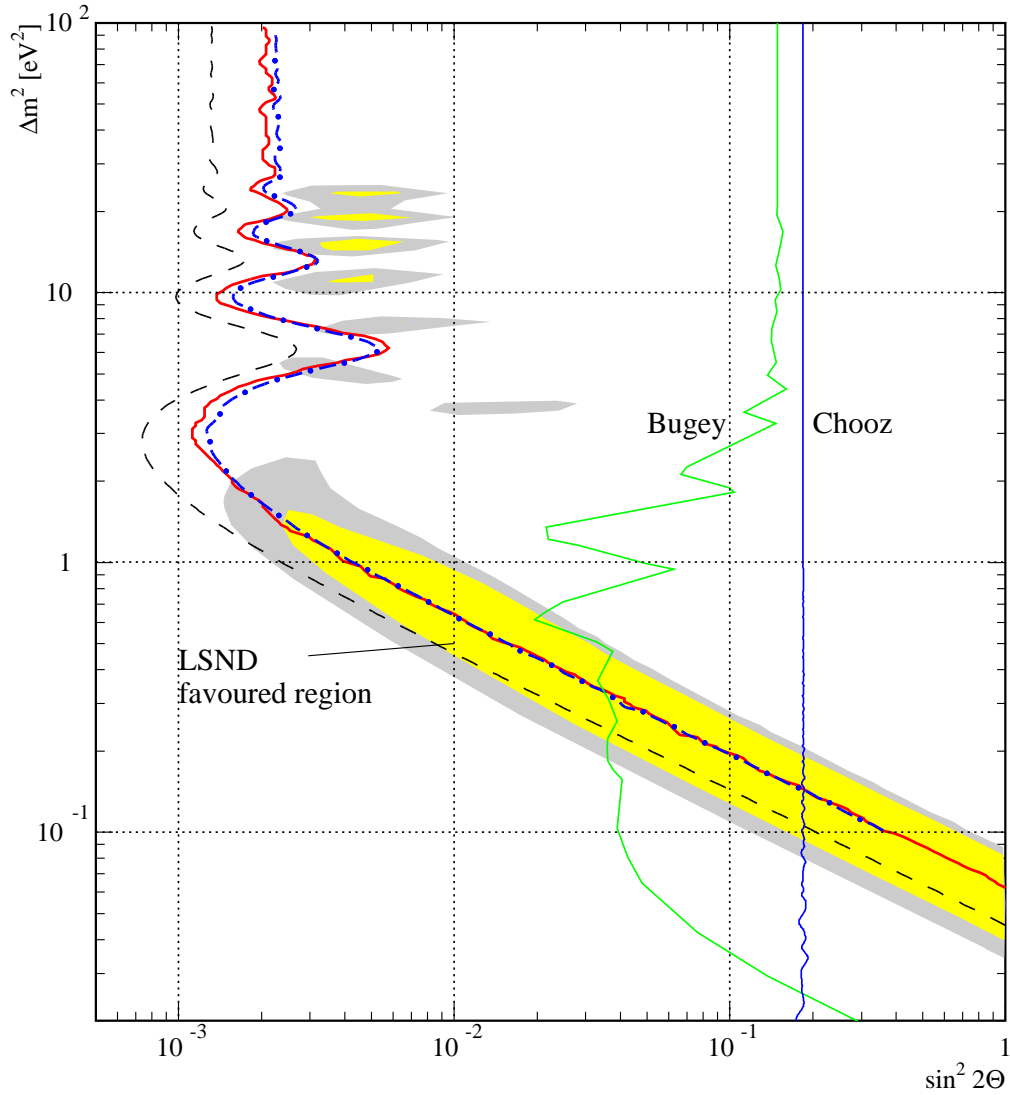


Figure 4: KARMEN 2 90% confidence limits according to the Unified Approach compared to other experiments: The full line is the 90% C.L. of the data presented here, the dotted line the corresponding sensitivity and the dashed line the 90% C.L. derived from the Feb. 97-Apr. 98 data. Also shown are the 90% C.L. of the two reactor experiments Chooz [14] and Bugey [15] and the favoured region for $\bar{\nu}_\mu \rightarrow \bar{\nu}_e$ oscillations as reported by the LSND experiment [11]. Areas to the right of the 90% C.L. are excluded with a probability of more than 90%. For the LSND result the “99% favoured region” (total shaded area) and the “90% favoured region” (light-shaded area) are given.

References

1. KARMEN collaboration:
 B. Armbruster, G. Drexlin, K. Eitel, H. Gemmeke, T.E. Jannakos, M. Kleifges, J. Kleinfeller, C. Oehler, P. Plischke, J. Rapp, M. Steidl, J. Wolf, B. Zeitnitz: *Forschungszentrum Karlsruhe, Institut für Kernphysik, Postfach 3640, D-76021 Karlsruhe, Germany*;
 B.A. Bodmann, E. Finckh, S. Haug, J. Hößl, P. Jünger, W. Kretschmer, I. Stucken: *Physikalisches Institut, Universität Erlangen-Nürnberg, Erwin Rommel Straße 1, D-91058 Erlangen, Germany*;
 C. Eichner, R. Maschuw, C. Ruf: *Institut für Strahlen- und Kernphysik, Universität Bonn, Nußallee 14-16, D-53115 Bonn, Germany*;
 I.M. Blair, J.A. Edgington: *Physics Department, Queen Mary and Westfield College, Mile End Road, London E1 4NS, United Kingdom*;
 N.E. Booth: *Department of Physics, University of Oxford, Keble Road, Oxford OX1 3RH, United Kingdom*
2. B. Zeitnitz *et al.*, Prog. Part. Nucl. Physics **40**, 169 (1998).
3. B. Armbruster *et al.*, Phys. Rev. C **57**, 3414 (1998).
4. R. Maschuw *et al.*, Prog. Part. Nucl. Physics **40**, 183 (1998).
5. B. Armbruster *et al.*, Phys. Rev. Lett. **81**, 520 (1998).
6. G.J. Feldman and R.D. Cousins, Phys. Rev. D **57**, 3873 (1998).
7. R.L. Burman *et al.*, Nucl. Instr. Meth. A **368**, 416 (1996).
8. G. Drexlin *et al.*, Prog. Part. Nucl. Physics **40**, 193 (1998).
9. R.M. Barnett *et al.* (Particle Data Group), Phys. Rev. D **54** 1 (1996).
10. M. Steidl, Thesis in preparation, Universität Karlsruhe 1999.
11. C. Athanassopoulos *et al.*, Phys. Rev. C **54**, 2685 (1996).
12. B. Zeitnitz *et al.*, to be publ. in Nucle. Phys. **B** Proceedings. hep-ex/9809007.
13. T.E. Jannakos, Thesis, Universität Karlsruhe 1998.
14. M. Appolonio *et al.*, Phys. Lett. B **420**, 397 (1998).
15. B. Achkar *et al.*, Nucl. Phys. B **434**, 503 (1995).